

Comparison of nonintensified and intensified CCD detectors for laser-induced breakdown spectroscopy

Jorge E. Carranza, Emily Gibb, Ben W. Smith, David W. Hahn, and James D. Winefordner

The performance and sensitivity of an intensified CCD array system and a nonintensified CCD array detector system are compared for laser-induced breakdown spectroscopy (LIBS). LIBS measurements were recorded in a calcium-based aerosol-seeded gas stream at ambient pressure. The signal-to-noise ratio based on the 393.37-nm calcium emission line was calculated as a function of detector delay with respect to the plasma-initiating laser pulse. Both ensemble-averaging and single-shot spectral analyses were performed. For all conditions, the intensified CCD system provided an enhanced signal-to-noise ratio compared with the nonintensified CCD system. © 2003 Optical Society of America

OCIS codes: 140.3440, 300.0300, 300.6210.

1. Introduction

A significant advantage of laser-induced breakdown spectroscopy (LIBS) is its ability to perform simultaneous analyses of multiple elements or multiple lines of the same element. To accomplish such measurements in real-time or in single-shot modes requires broadband spectral detectors. Since the advent of the LIBS technique, a variety of detector types have been employed. The most frequently used have been optical multichannel analyzers, photodiode array detectors, and both nonintensified charge-coupled devices (CCDs), including linear and two-dimensional configurations, and intensified CCD (ICCD) arrays. Of these detectors, the ICCD array has probably been the most studied for LIBS applications, including recent investigations of sensitivity and shot-to-shot variations.^{1,2} As discussed in the following paragraphs, detector choices for LIBS depend on many factors, including data acquisition rates and type of signal processing (e.g., single-shot or ensemble averaging), required analyte sensitivity, spectral bandwidth, field deployability, and overall system cost.

The ICCD has served as the detector platform for a great variety of LIBS applications, including some of the most recent studies in the quantitative analysis of artwork³ and of molten alloys.⁴ In these applications ensemble-averaged spectra were used to smooth the pulse-to-pulse variations frequently seen in LIBS. In contrast, in applications such as those that require rapid sorting or for which it is desirable to see emission from a single particle, single-shot spectra are required. Studies have reported single-shot spectral analysis to yield quantitative information for thin films of Fe–Ni alloys produced by pulsed laser desorption.⁵ In the field of aerosol science, the size and composition of ambient aerosol particles were determined by single-shot spectral analysis.⁶

The use of non-ICCD arrays in LIBS is less prevalent, with the majority of such applications focused on analysis of solid samples. Correlation analysis was successfully implemented in the identification of stainless-steel standards with a non-ICCD array in combination with a microscopic LIBS system.⁷ The correlation principle was later extended to the generation of calibration curves based on linear correlation of ensemble-averaged spectral intensities. These calibration curves facilitated quantitative analyses of the amount of copper in brass standards and of aluminum, silicon, and copper in aluminum alloy standards.⁸ Improvements in precision of the LIBS signal for magnesium were obtained by use of a surface density normalization technique in a traditional LIBS setup, achieving ~10% relative error in a variety of sample matrices.⁹ Nonintensified systems are advantageous because of their ability to be integrated into portable LIBS systems. An applica-

The authors are with the University of Florida, Gainesville, Florida 32611. J. E. Carranza and D. W. Hahn (dwhahn@ufl.edu) are with the Department of Mechanical and Aerospace Engineering. E. Gibb, B. W. Smith, and J. D. Winefordner are with the Department of Chemistry.

Received 17 February 2003; revised manuscript received 24 June 2003.

0003-6935/03/306016-06\$15.00/0

© 2003 Optical Society of America

Table 1. System Specifications

Parameter	ICCD System	CCD System
Spectrometer model	Acton Research 300i	Ocean Optics HR2000
Detector model	Princeton Instruments PI-Max 1024RB	Ocean Optics HR2000
Grating	1200 g/mm holographic	2400 g/mm holographic
Entrance slit (μm)	10	5
Linear dispersion (nm/pixel)	0.06	0.05
Optical resolution (nm)	0.18	0.15
CCD format	1024 \times 256	2048 \times 1
Pixel size (μm)	26 \times 26	12.5 \times 200
Readout rate	100 kHz	1 MHz
Intensifier	25-mm Gen II	
CCD cooling	-20 $^{\circ}\text{C}$	Ambient

tion that demonstrated the implementation of such a field-portable LIBS system was the on-line sorting of waste wood treated with chromated copper arsenate (CCA), which yielded 92–100% accurate identification of the CCA-treated wood.¹⁰ Non-ICCD detectors are appearing more frequently in research laboratories because of the much lower costs of those detectors than of the ICCD systems. With many recent applications of both ICCD and CCD systems for LIBS analysis it is useful to compare the relative performance of these two detector types. A recent study addressed this issue for the LIBS-based analysis of solid samples.¹¹ Our goal in this paper is to compare the sensitivity and performance of an intensified CCD array and a non-ICCD array for both ensemble-averaging and single-shot LIBS analysis.

2. Experimental System and Methodology

A brief description of the LIBS experimental setup and the sample-generation system is presented here; complete details were reported in a previous paper.¹² A 1064-nm *Q*-switched Nd:YAG laser operating with 290-mJ pulse energy, 10-ns pulse width, and 5-Hz pulse repetition rate was used as the laser-induced plasma source. The laser beam was expanded to 12-mm diameter and focused in the sample stream by a 75-mm focal-length UV-grade plano-convex lens. The plasma emission was collected along the incident beam in a backward direction (180 $^{\circ}$) and separated with a 50-mm-diameter UV-enhanced pierced mirror. The collected light was launched into a 1-mm-diameter multimode optical fiber, which was used to couple the plasma emission to either of two spectrometer-detector systems.

Two spectrometer-detector systems were investigated: an ICCD array detector coupled to a 0.3-m spectrometer and a linear CCD array detector integrated into a compact, high-resolution Czerny-Turner spectrometer. The former system is referred to here as the ICCD system; the latter, the CCD system. Complete details of the two systems are summarized in Table 1. Because our goal in this paper is to compare directly the performance of these two systems for LIBS-based analysis, care was taken to match the input parameters with respect to the plasma emission.

The 1-mm optical fiber was directly coupled to the CCD system through a 5- μm entrance slit, which yielded an effective fiber delivery area of 0.005 mm². The entrance slit of the ICCD system was configured for a different type of fiber termination from that of the 1-mm optical fiber; hence the 1-mm fiber was subsequently coupled to a fiber optic bundle that was configured with the correct termination. The fiber optic bundle consisted of 19 individual 200- μm optical fibers arranged in a circular bundle at the input end and arranged in a linear array for coupling to the 10- μm spectrometer entrance slit. By using the 1-mm fiber optic for coupling to the plasma emission collection optics for all experiments we maintained a constant source of plasma emission. After fiber-to-fiber coupling, only 5 of the 19 optical fibers were observed to be strongly illuminated with plasma emission. To prevent detector saturation of the ICCD readout array we selected and binned approximately 50 rows, corresponding to only 2 of the illuminated optical fibers, for all experiments. The effective fiber delivery area for the ICCD system was 0.004 mm², based on the slit width and diameter of the two fibers analyzed. Based on a measured fiber-to-fiber coupling efficiency of 30%, the fraction of illuminated fibers used (2/5), and the ratio of effective fiber delivery areas, we estimate that the ICCD system was coupled to \sim 10% of the amount of plasma emission that was coupled to the CCD system.

Because LIBS measurements are generally performed with temporal signal gating, various delays with respect to the incident laser pulse were explored. For both systems, a digital delay generator was used to provide an external trigger to the detector with a specified delay with respect to the plasma-initiating laser pulse ($t = 0$). By triggering from the laser flash lamp, the delay generator output was adjusted until a given detector system was triggered coincidentally with the laser pulse. This zero delay was stored for each system and accounted for all internal delays inherent in each system when it is being operated in the external trigger mode. LIBS spectra were subsequently recorded for each system by use of introduced delays of 1, 2, 3, 5, 10, 20, and 30 μs with respect to the incident laser pulse. The CCD system was characterized by a fixed minimum integration of

the order of 1 ms for all experiments. For comparison, the ICCD was operated with a fixed detector gate width of 250 μs , controlled by the intensifier gate, for all experiments. The detector gate widths of 1 ms and 250 μs were both much longer than the plasma decay time; hence both systems effectively integrated the entire plasma emission following the specified initial delays. This integration mitigated any effects that resulted from the true gating capabilities (i.e., detector delay and gate width control) of the ICCD and the external triggering capabilities (i.e., detector delay control only) of the CCD system. The overall temporal jitter between the laser pulse and initiation of detector integration was of the order of 1 ns for the ICCD system and of the order of 100 ns for the CCD system.

The CCD system was operated with a preset fixed gain and with a corresponding full-scale value of 4095 counts (12-bit resolution). The ICCD system was operated with a variable gain that corresponded to the intensifier voltage setting. The intensifier voltage setting was digitized with 8-bit resolution, yielding a range from 1 to 256 for the intensifier gain scale, with a value of 1 corresponding to the minimum intensifier voltage. The single-pixel dynamic range was defined by 16-bit resolution, providing a full-scale reading of 65,535 counts. For the ICCD system, the intensifier gain was maintained constant at the minimum setting (gain of 1) for delay times of 1, 2, 3, and 5 μs , after which the gain was adjusted to maintain continuum-resolved signal levels for delay times of 10, 20, and 30 μs .

All experiments were performed in a gaseous sample stream that comprised filtered, dry air seeded with a submicrometer-sized calcium-based aerosol. The sample stream was prepared by the nebulization of an aqueous solution of calcium (ICP-grade standard at 10,000- $\mu\text{g}/\text{mL}$ calcium) into a gaseous coflow stream of 42-L/min air. The nebulizer functioned to produce a well-dispersed aerosol stream of calcium-based nanoparticles following droplet evaporation, with a mean particle size of ~ 100 nm and a corresponding particle number density near 10^6 cm^{-3} .¹² The resultant aerosol-laden sample stream presented a well-controlled and well-dispersed system for LIBS-based data acquisition. For each delay time and detector system, a series of 200 single-shot spectra was recorded and saved.

Following data collection, LIBS-based analysis for all experiments used the Ca II (ionic) atomic emission lines at 393.37 and 396.85 nm. The data analysis was based on the signal-to-noise ratio (SNR) to quantify the calcium atomic emission lines. For the present analysis the SNR is defined as the ratio of the integrated atomic emission line intensity (peak area) to the average peak noise. The average peak noise was calculated by use of the rms of the adjacent, featureless continuum intensity times the full peak width; hence the reported SNR is dimensionless. The rms noise was determined from the deviation of a least-squares fit over a narrow spectral region corresponding to ~ 20 pixels. This procedure was per-

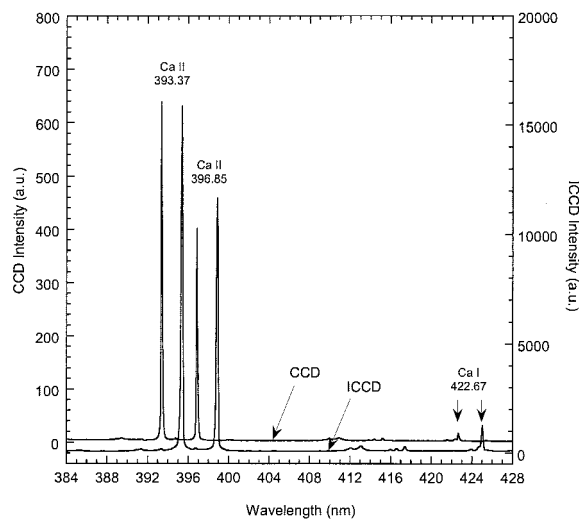


Fig. 1. LIBS spectra corresponding to an ensemble average of 200 laser shots recorded with an ICCD and with a CCD system at a delay time of 5 μs . The ICCD spectrum has been shifted by 2 nm for clarity.

formed on both sides of the analyte emission line, and the results were averaged. The full line widths were based on 9 pixels for the CCD system and 8 pixels for the ICCD system. For a given delay, the SNR value was calculated for each individual spectrum, with the individual values then averaged to yield an average SNR value for single-shot analysis. These values are referred to as single-shot SNRs. In addition, all 200 collected spectra were ensemble averaged for each delay, and the resultant spectrum was used to calculate the SNR value. These values are referred to as the ensemble-averaged SNRs. These calculations were repeated for both the ICCD and the CCD systems for each corresponding delay time.

3. Results and Discussion

For comparison, the ICCD and the CCD systems were assessed first with respect to their performance for ensemble-averaged analysis and then for single-shot analysis. The ensemble-averaged spectra of 200 laser shots for the CCD and the ICCD systems are shown in Fig. 1 for a delay time of 5 μs . The delay of 5 μs corresponded to the optimal delay setting for both systems with ensemble averaging. For Fig. 1 and subsequent figures we shifted the ICCD spectrum uniformly by 2 nm to clarify the features of both spectra. The two spectra show similar features in the selected spectral window of 384–388 nm; the visibility of the calcium neutral atomic emission line (Ca I, 422.67 nm) and ionic emission lines (Ca II, 393.37 and 396.85 nm) is due to the calcium-based aerosols. In addition, a relatively noise-free continuum structure is present for both spectra, demonstrating a marked SNR for this optimal temporal delay. However, the major difference between the ICCD and the CCD ensemble-averaged spectra lies in the magnitude of the spectral intensities. The ICCD spectrum is characterized by calcium emission inten-

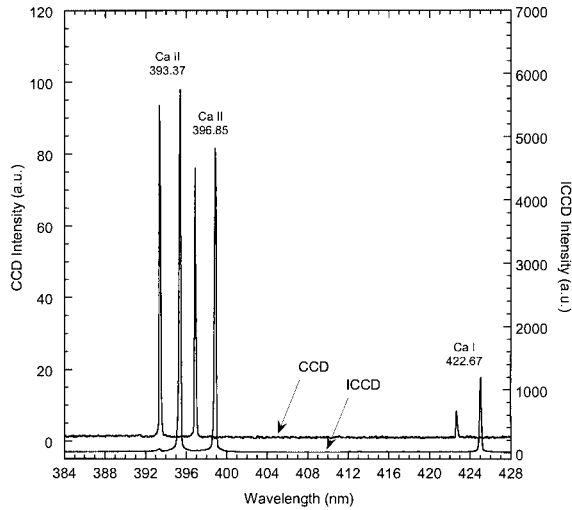


Fig. 2. LIBS spectra corresponding to an ensemble average of 200 laser shots recorded with an ICCD and with a CCD system at a delay time of 20 μs . The ICCD spectrum has been shifted by 2 nm for clarity.

sities that are 1 order of magnitude above those of the CCD spectrum despite the reduced plasma-emission coupling efficiency of the ICCD (it is 10% that of the CCD) and the minimum intensifier gain setting. Similarly, the continuum intensity is reduced from ~ 50 to 5 counts for the ICCD and the CCD spectra, respectively. A further discussion of the continuum is presented below. Similar behavior is shown in Fig. 2, where the ensemble-averaged spectra of the ICCD and the CCD are compared for a delay time of 20 μs . By 20 μs following the plasma initiation, both spectra are characterized by a marked decrease in calcium emission intensity. Despite the significant reduction in signal intensity, the ratio of the ICCD to the CCD emission intensity remains ~ 1 order of magnitude. Visual inspection of the spectra in Figs. 1 and 2 indicates that the ICCD system is characterized by a greater SNR than that of the CCD system. This observation is quantified in the following paragraphs.

An assessment of the performance of the ICCD and the CCD systems for single-shot analysis is presented in Figs. 3 and 4. Typical single-shot spectra that correspond to delay times of 5 and 20 μs are presented in Figs. 3 and 4, respectively. Consistent with the ensemble-averaged spectra, the ICCD data are characterized by an order-of-magnitude greater emission intensity than in the CCD system. In addition, it was observed that the relative spectral noise in the CCD spectra is higher than that in the ICCD spectra for both the 5- and the 20- μs time delays.

To quantify the direct comparison of the two systems, we calculated the SNRs for all delay times; they are presented in Fig. 5. The results demonstrate that the SNR values of the ICCD spectral data are greater than for the CCD system over all time delays for both ensemble-average and single-shot analyses. As shown in Fig. 5, the SNR ratio is maximized at ~ 5

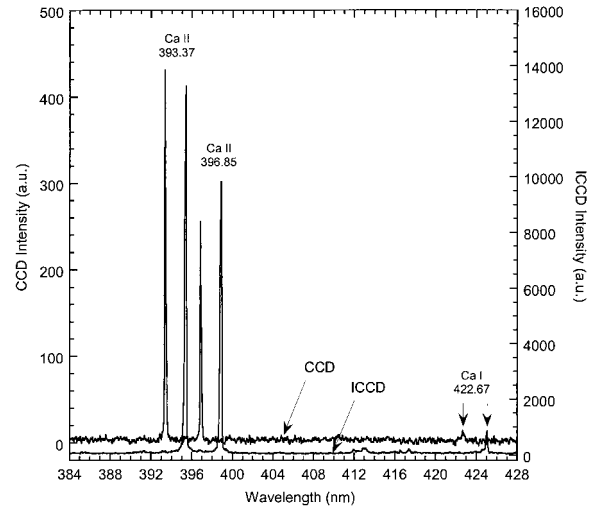


Fig. 3. Single-shot LIBS spectra recorded with an ICCD and with a CCD system at a delay time of 5 μs . The ICCD spectrum has been shifted by 2 nm for clarity.

μs for both systems and processing schemes. The increase in the SNR from the CCD to the ICCD system ranged from 3.5-fold at a 5- μs delay to nearly 25-fold at a 1- μs delay for ensemble averaging. For single-shot processing, the increase in the ICCD ranged from 2.8-fold at 3- μs delay to ~ 25 -fold at 30- μs delay. Overall, the ICCD system enjoys an approximate factor-of-3 improvement compared with the CCD system in SNR, and hence in the limit of detection, at the optimal delay time and a more than 1-order-of-magnitude improvement at longer delay times. These conclusions are consistent with the recent results of Sabsabi *et al.*; they found the limits of detection of an ICCD system to be better than those of a CCD system by more than 1 order of magnitude

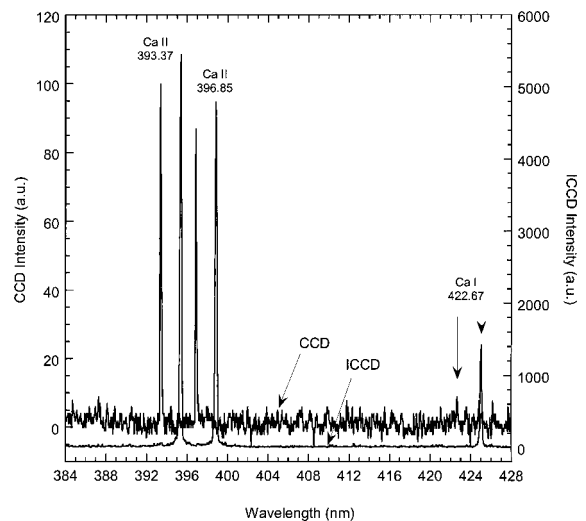


Fig. 4. Single-shot LIBS spectra recorded with an ICCD and with a CCD system at a delay time of 20 μs . The ICCD spectrum has been shifted by 2 nm for clarity.

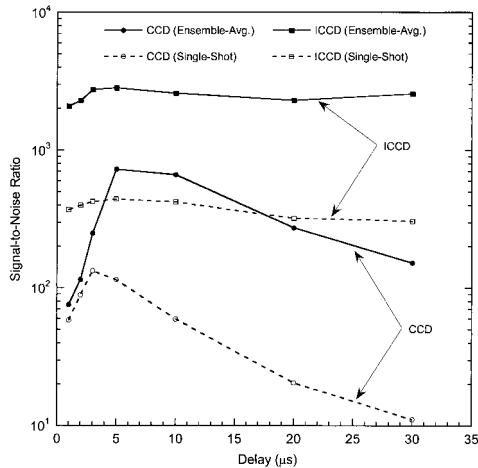


Fig. 5. SNR of the 393.37-nm Ca II emission line as a function of delay time for the ICCD and the CCD systems, obtained from both ensemble-averaged and single-shot spectral analyses.

for detection of beryllium, copper, magnesium, and manganese in standard aluminum solids.¹¹

Note that the Ca II lines are characterized by relatively short optimal delay times, whereas neutral emission lines of other elements such as lead and chromium have optimal delay times of tens of microseconds under similar laser-induced plasma conditions.¹³ Therefore it is difficult to extrapolate the specific performance differences between the two systems to additional elements. Nonetheless, the rapid decrease in SNR with increasing delay time of the CCD system in contrast to the ICCD system suggests that the CCD system is better suited to temporal regimes relatively close to plasma initiation. In addition to temporal considerations, the current research was limited to a spectral region near 400 nm. Additional comparisons at other spectral regions, such as the UV and the near IR, should also take into account the range of quantum efficiencies of the relevant detector systems.

It is also useful to examine the plasma continuum intensity recorded with the two systems. Because of the generally large shot-to-shot fluctuations that are characteristic of LIBS, most spectral processing is done with a peak-to-continuum (i.e., peak-to-base) ratio. Once the continuum emission intensity falls below the detection threshold, despite the persistence of analyte atomic emission peaks, additional experimental uncertainty is introduced for quantitative analysis as a result of the inability to normalize spectra.² As shown in Figs. 1–4, the continuum is characterized by relatively low intensities and is difficult to discern relative to the analyte emission peaks. The continuum emission intensity for a narrow spectral region is presented in Fig. 6 for delay times of 3 and 5 μ s. This temporal regime corresponds to the rapid drop in continuum intensity as measured with the CCD system. As revealed in Fig. 6, the ICCD spectra show characteristic features that correspond

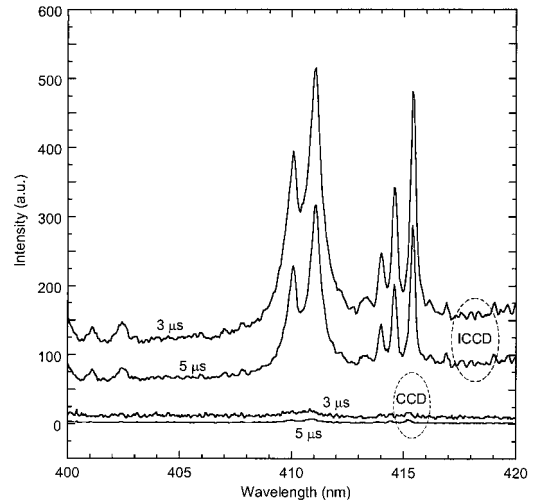


Fig. 6. Ensemble-averaged plasma continuum emission recorded with the ICCD and the CCD systems for delay times of 3 and 5 μ s.

to the atomic emission lines of nitrogen (\sim 410 nm) and oxygen (\sim 415 nm) in addition to a strong continuum background. In contrast, the CCD spectra are characterized by a diminished response and do not resolve the spectral features as observed in the ICCD spectra. The CCD spectrum that corresponds to 5- μ s delay is essentially detector noise. The ICCD detector successfully recorded the continuum emission for all delay times, including 30 μ s.

In summary, a careful comparison of ICCD and CCD systems for LIBS analysis revealed significant differences in performance, as quantified by the SNR and the ability to record plasma continuum emission. The ICCD system yielded better performance for both ensemble-averaged and single-shot analyses, with improvements in SNR ranging from a factor of 3 to greater than 1 order of magnitude compared with the CCD system. In addition, the relatively weak continuum signal achieved with the CCD system for moderate temporal delays might affect single-shot measurements if peak-to-continuum normalization is desirable. Ultimately, the choice of detector for a given LIBS application should encompass many parameters, including the required analyte sensitivity, the signal-processing modes (e.g., single shot or ensemble averaging), the necessary spectral bandwidth, and issues of field deployability and overall system cost. Clearly, both intensified and non-intensified CCD detector arrays are practical technologies, which provide the LIBS researcher with a range of detector options to match specific applications.

The authors are grateful to Roy Walters of Ocean Optics, Inc., for readily making available the HR2000 CCD system.

References

1. B. C. Castle, K. Talabardon, B. W. Smith, and J. D. Winefordner, "Variables influencing the precision of laser-induced

- breakdown spectroscopy measurements," *Appl. Spectrosc.* **52**, 649–657 (1998).
2. J. E. Carranza and D. W. Hahn, "Sampling statistics and considerations for single-shot analysis using laser-induced breakdown spectroscopy," *Spectrochim. Acta Part B* **57**, 779–790 (2002).
 3. F. Colao, R. Fantoni, V. Lazic, and V. Spizzichino, "Laser-induced breakdown spectroscopy for semi-quantitative and quantitative analyses of artworks—application on multi-layered ceramics and copper based alloys," *Spectrochim. Acta Part B* **57**, 1219–1234 (2002).
 4. A. R. Rai, F. Y. Yueh, J. P. Singh, and H. Zhang, "High temperature fiber optic laser-induced breakdown spectroscopy sensor for analysis of molten alloy constituents," *Rev. Sci. Instrum.* **73**, 3589–3599 (2002).
 5. C. Aragón, V. Madurga, and J. A. Aguilera, "Application of laser-induced breakdown spectroscopy to the analysis of the composition of thin films produced by pulsed laser desorption," *Appl. Surface Sci.* **197-198**, 217–223 (2002).
 6. J. E. Carranza, B. T. Fisher, G. D. Yoder, and D. W. Hahn, "On-line analysis of ambient aerosols using laser-induced breakdown spectroscopy," *Spectrochim. Acta Part B* **56**, 851–864 (2001).
 7. I. B. Gornushkin, B. W. Smith, H. Nasajpour, and J. W. Winefordner, "Identification of solid materials by correlation analysis using a microscopic laser-induced plasma spectrometer," *Anal. Chem.* **71**, 5157–5184 (1999).
 8. G. Galbács, I. B. Gornushkin, B. W. Smith, and J. D. Winefordner, "Semi-quantitative analysis of binary alloys using laser-induced breakdown spectroscopy and a new calibration approach based on linear correlation," *Spectrochim. Acta Part B* **56**, 1159–1173 (2001).
 9. S. I. Gornushkin, I. B. Gornushkin, J. M. Anzano, B. W. Smith, and J. D. Winefordner, "Effective normalization technique for the correction of matrix effects in laser-induced breakdown spectroscopy detection of magnesium in powdered samples," *Appl. Spectrosc.* **56**, 433–436 (2002).
 10. T. M. Moskal and D. W. Hahn, "On-line sorting of wood treated with chromated copper arsenate using laser induced breakdown spectroscopy," *Appl. Spectrosc.* **56**, 1337–1344 (2002).
 11. M. Sabsabi, R. Heon, V. Detalle, L. St-Onge, and A. Hamel, "Comparison between intensified CCD and non-intensified gated CCD detectors for LIPS analysis of solid samples," in *Laser Induced Plasma Spectroscopy and Applications*, Vol. 81 of OSA Trends in Optics and Photonics Series (Optical Society of America, Washington, D.C., 2002), pp. 128–130.
 12. D. W. Hahn, J. E. Carranza, G. R. Arsenault, H. A. Johnsen, and K. R. Hencken, "Aerosol generation system for development and calibration of laser-induced breakdown spectroscopy instrumentation," *Rev. Sci. Instrum.* **72**, 3706–3713 (2001).
 13. B. T. Fisher, H. A. Johnsen, S. G. Buckley, and D. W. Hahn, "Temporal gating for the optimization of laser-induced breakdown spectroscopy detection and analysis of toxic metals," *Appl. Spectrosc.* **55**, 1312–1319 (2001).